IRTA
RECERCA | TECNOLOGIA AGROALIMENTÀRIES

This document is a postprint version of an article published in Veterinary Microbiology © Elsevier after peer review. To access the final edited and published work see https://doi.org/10.1016/j.vetmic.2020.108744.

Document downloaded from:

IRTA Pubpro
Open digital archive

Title

Activation of pro- and anti-inflammatory responses in lung tissue injury during the acute phase of PRRSV-1 infection with the virulent strain Lena

Sánchez-Carvajal J.M.[a,*], Rodríguez-Gómez I.M.[a], Ruedas-Torres I.[a], Larenas-Muñoz F.[a] Díaz I.[b], Revilla C.[c], Mateu E.[b,d], Domínguez J.[c], Martín-Valls G.[d], Barranco I.[a], Pallarés F.J.[e], Carrasco L.[a], Gómez-Laguna J.[a]

[a]Department of Anatomy and Comparative Pathology, Faculty of Veterinary Medicine, University of Córdoba, 14014, Córdoba, Spain

[b]Institut de Recerca i Tecnologia Agroalimentàries - Centre de Recerca en Sanitat Animal (IRTA-CReSA), Campus de la Universitat Autònoma de Barcelona, 08193 Cerdanyola del Vallès, Spain.

[c]Department of Biotechnology, National Institute for Agricultural and Food Research and Technology (INIA), 28040, Madrid, Spain

[d]Department of Animal Health and Anatomy, Faculty of Veterinary Medicine, Autonomous University of Barcelona, 08193, Bellaterra, Spain

[e]Department of Anatomy and Comparative Pathology, Faculty of Veterinary Medicine, University of Murcia, 30100, Murcia, Spain

*Corresponding author at: Department of Anatomy and Comparative Pathology, Faculty of Veterinary Medicine, University of Córdoba, 14014, Córdoba, Spain.

E-mail address: v42sancj@uco.es (J.M. Sánchez-Carvajal).

Abstract (250 words)

Porcine reproductive and respiratory syndrome virus (PRRSV) plays a key role in porcine respiratory disease complex modulating the host immune response and favouring secondary bacterial infections. Pulmonary alveolar macrophages (PAMs) are the main cells supporting PRRSV replication, with CD163 as the essential receptor for viral infection. Although interstitial pneumonia is by far the representative lung lesion, suppurative bronchopneumonia is described for PRRSV virulent strains. This research explores the role of several immune markers potentially involved in the regulation of the inflammatory response and sensitisation of lung to secondary bacterial infections by PRRSV-1 strains of different virulence. Conventional pigs were intranasally inoculated with the virulent subtype 3 Lena strain or the low virulent subtype 1 3249 strain and euthanised at 1, 3, 6 and 8 dpi. Lena-infected pigs exhibited more severe clinical signs, macroscopic lung score and viraemia associated with an increase of IL-6 and IFN-γ in sera compared to 3249-infected pigs. Extensive areas of lung consolidation corresponding with suppurative bronchopneumonia were observed in Lena-infected pigs. Lung viral load and PRRSV-N-protein$^+$ cells were always higher in Lena-infected animals. PRRSV-N-protein$^+$ cells were linked to a marked drop of CD163$^+$ macrophages. The number of CD14$^+$ and iNOS$^+$ cells gradually increased along PRRSV-1 infection, being more evident in Lena-infected pigs. The frequency of CD200R1$^+$ and FoxP3$^+$ cells peaked late in both PRRSV-1 strains, with a strong correlation between CD200R1$^+$ cells and lung injury in Lena-infected pigs. These results highlight the role of molecules involved in the earlier and higher extent of lung lesions in piglets infected with the virulent Lena strain, pointing out the activation of routes potentially involved in the restraint of the local inflammatory response.

Keywords: *PRRSV-1, virulent strains, lung lesion, inflammatory response*

Introduction

Porcine reproductive and respiratory syndrome virus (PRRSV) encompasses two species, *Betaarterivirus suid 1* and *Betaarterivirus suid 2* (formerly, PRRSV-1 and PRRSV-2, respectively) (Gorbalenya et al., 2018), which present a wide inter- and intra-species viral diversity (Balka et al., 2018; Shi et al., 2010; Stadejek et al., 2013). Since 2006, different outbreaks characterised by high morbidity and mortality rates, fever, haemorrhages, severe lesions in lung and, eventually, in other organs such as thymus or lymph nodes, have been reported associated with virulent PRRSV-1 strains (Canelli et al., 2017; Karniychuk et al., 2010; Morgan et al., 2013, 2016; Ogno et al., 2019; Sinn et al., 2016; Weesendorp et al., 2013). Several contradictory results about viraemia, tissue viral load, early virus clearance, low frequencies of PRRSV-specific IFN-γ secreting cells or PRRSV neutralizing antibodies have been reported after infection with PRRSV-1 virulent strains. However, there is consensus on the fact that some strains are more virulent than others (Canelli et al., 2017; Ferrari et al., 2018; Frydas et al., 2013; Geldhof et al., 2012; Morgan et al., 2013; Renson et al., 2017; Stadejek et al., 2017; Weesendorp et al., 2013, 2014).

PRRSV replicates predominantly in the lung, causing a mild to severe interstitial pneumonia which may be complicated to suppurative bronchopneumonia due to the increased lung sensitisation to bacterial infections associated with the damage and impairment of the different pulmonary macrophage subpopulations (pulmonary alveolar macrophages, PAMs; pulmonary intravascular macrophage, PIMs; and interstitial macrophages) (Brockmeier et al., 2017; Thanawongnuwech et al., 2000). PAMs are the main cellular target of PRRSV, although interstitial and intravascular macrophages can be infected too (Bordet et al., 2018; Duan et al., 1997; Gómez-Laguna et al., 2010), with

the nucleocapsid protein N (PRRSV-N-protein) as the most abundant viral protein during PRRSV infection (Rowland et al., 1999). PAMs express high levels of CD163 scavenger receptor (Sánchez et al., 1999; Van Gorp et al., 2008) which is essential to support PRRSV internalisation and disassembly interacting with GP2 and GP4 viral proteins (Burkard et al., 2017; Das et al., 2010; Whitworth et al., 2016). A soluble form of CD163 (sCD163), that may be released from tissue macrophages and monocytes, has been identified in plasma as potential biomarker for macrophage activity and inflammation (Costa-Hurtado et al., 2013; Møller, 2012; Pasternak et al., 2019).

PRRSV is known to modulate the host immune response by inducing changes in the frequencies of immune cell subsets in blood (Dwivedi et al., 2012; Ferrari et al., 2018; Morgan et al., 2013; Weesendorp et al., 2013) and in tissues (Gómez-Laguna et al., 2010; Rodríguez-Gómez et al., 2013), leading to an enhanced susceptibility to secondary bacterial infections (Karniychuk et al., 2010; Renson et al., 2017; Sinn et al., 2016). An early decrease in the frequency of monocytes, NK cells or cytotoxic T cells linked to a strong inflammatory response in target organs has been described upon experimental infection with PRRSV-1 virulent strains (Ferrari et al., 2018; Morgan et al., 2013; Weesendorp et al., 2013; 2014). In addition, some studies indicate an early overproduction of pro-inflammatory cytokines, such as IFN-γ, IL-1β or IL-8, as the main source of pulmonary injury after infection with virulent PRRSV-1 strains (Amarilla et al., 2015; Morgan et al., 2013; Renson et al., 2017; Weesendorp et al., 2014). Nevertheless, other potential mechanisms, such as an imbalance among pro- and anti-inflammatory responses, might predispose to secondary infections contributing to the onset of the porcine respiratory disease complex (PRDC) (Gómez-Laguna et al., 2013; Van Gucht et al., 2004).

In this context, overproduction of nitric oxide (NO), mainly triggered by inducible NO synthase (iNOS) (Akaike and Maeda, 2000), or upregulation of CD14, as the primary lipopolysaccharide (LPS) receptor (Zanoni and Granucci, 2013), could contribute to lung inflammation upon infection with PRRSV (Chen et al., 2014; Lee and Kleiboeker, 2005; Van Gucht et al., 2004, 2005; Yan et al., 2017). By contrast, the transcription factor forkhead box protein 3 (FoxP3), is an essential transcription factor for the development of regulatory T cells (Tregs) and hence, a useful marker to detect them. This subset could be involved in supressing the activation of other T-cell populations (Käser et al., 2008). CD200 receptor 1 (CD200R1), expressed on myeloid cells and B cell subsets (Poderoso et al., 2019), is an inhibitory surface receptor that might deliver inhibitory signals dampening the activation of cells which express it (Vaine and Soberman, 2014). Thus, both immune markers might play an important role inhibiting the production of pro-inflammatory cytokines (Elmore et al., 2014; Nedumpun et al., 2018; Singh et al., 2019; Vaine and Soberman, 2014; Wang et al., 2018), lessening the exuberant lung injury observed with virulent PRRSV-1 strains. Whereas all these markers may play a key role in PRRSV virulence, there are scarce studies analysing their role in the context of the lung lesion. Therefore, the systemic immune response and immunopathology of lung are evaluated in this study with the goal of exploring the role of selected immune markers in the pro- and anti-inflammatory priming of the lung to secondary bacteria after infection with a virulent PRRSV-1 strain (subtype 3, Lena strain) in comparison with a low virulent PRRSV-1 strain (subtype 1, 3249 strain).

2. Materials and methods

2.1. Porcine reproductive and respiratory syndrome strains

The low virulent 3249 strain (subtype 1 PRRSV-1) was isolated from the serum of a piglet with pneumonia from a PRRSV-positive herd located in Spain in 2005 (Gimeno et al., 2011). The virulent Lena strain (subtype 3 PRRSV-1) is considered as the prototype of PRRSV-1 virulent strains. Lena strain isolation was performed from lung homogenates obtained from weak born piglets from a PRRSV-positive herd from Belarus in 2007 with a high mortality rate, reproductive failure and respiratory disorders (Karniychuk et al., 2010). Viral stocks were produced from the 4^{th} passage of each strain on PAMs, titrated by means of immunoperoxidase monolayer assay and expressed as tissue culture infectious doses 50 ($TCID_{50}$)/mL (3249 strain: $10^{5.79}$ $TCID_{50}$/mL; Lena strain: $10^{5.66}$ $TCID_{50}$/mL).

2.2. Animals and experimental design

The animals and samples used in this study were part of a project to investigate the pathogenesis of the infection with PRRSV-1 strains of different virulence (Rodríguez-Gómez et al., 2019). Briefly, fifty-two 4-week-old male and female piglets (Landrace x Large White crossbred) were obtained from a historically PRRSV-negative farm. All pigs were negative for porcine circovirus type 2 (PCV2), PRRSV and *Mycoplasma hyopneumoniae* by ELISA and PCR assays (Mattsson et al., 1995; Sibila et al., 2004).

Piglets were blocked by weight and sex and randomly assigned to three different groups and housed in separate pens: Lena group (n=20), 3249 group (n=20) and control group (n=12). After an acclimation period of seven days, piglets were intranasally inoculated with either the low virulent 3249 strain or the virulent Lena strain (both used at $1x10^5$ $TCID_{50}$/mL, 1 mL/nostril, using the MAD Nasal™ Intranasal Mucosal Atomization Device, Teleflex, Alcalá de Henares, Madrid, Spain). The control group was mock-

inoculated with the PAM supernatant diluted with RPMI similarly to the inoculum. Three control pigs and five infected pigs from each group were euthanised on days 1, 3, 6 and 8 post-inoculation (dpi). This experiment was conducted according to the guidelines of the European Union (Directive 2010/63/EU) and approved by the IRTA Ethics Committee and by the Catalan Autonomous Government (Project 3647; FUE-2017-00533413).

2.3. Clinical signs, gross pathology and histopathology of lung

Commencing 1 day prior to inoculation, piglets were daily monitored to evaluate clinical signs (liveliness, respiratory symptoms and anorexia) and rectal temperature. Quantification of clinical signs was performed by applying the following clinical score: liveliness (score 0, no abnormalities; score 1, reduced liveliness but with response to external stimuli; score 2, pig prostration; score 3, agonic pig); respiratory symptoms (score 0, no abnormalities; score 1, mild dyspnoea; score 2, evident dyspnoea; score 3, evident dyspnoea with tachypnoea; score 4, evident dyspnoea, tachypnoea and cyanosis); and anorexia (score 0, eating without abnormality; score 1, sporadic frequency of eating; score 2, no eating). The sum of these scores represented the total clinical score per animal and per day. Rectal temperatures > 40.5 °C were considered hyperthermia. At necropsy, gross lung lesions were recorded and scored by the same pathologist (Halbur et al., 1996). Afterwards, samples from apical, medial and caudal lobes from the right lung were collected and fixed in 10 % neutral-buffered formalin (Fisher Scientific Ltd., Loughborough, UK) for histopathological and immunohistochemical studies.

Four-micron tissue sections were stained with haematoxylin and eosin and blindly graded by two pathologists for the histopathological evaluation. The severity of histopathological

lesions in the lung was scored as previously described by Halbur et al. (1996): 0, no microscopic lesions; 1, mild interstitial pneumonia; 2, moderate multifocal interstitial pneumonia; 3, moderate diffuse interstitial pneumonia; and 4, severe interstitial pneumonia. In addition, a similar score was developed considering the diagnosis of suppurative bronchopneumonia (Rodríguez-Gómez et al., 2019): 0, no microscopic lesions; 1, mild bronchopneumonia; 2, moderate multifocal bronchopneumonia; 3, moderate diffuse bronchopneumonia; and 4, severe bronchopneumonia. Altogether, the final score included the total of both, the interstitial pneumonia score and the bronchopneumonia score, being 8 points the maximum possible score.

2.4. Viral genome quantification

RNA was isolated from sera using NucleoSpin® RNA virus (Macherey-Nagel, Düren, Germany) according to manufacturer's instructions. For lung, RNA was purified from tissue homogenate using a combined procedure with TRIzol™ (Thermo Fisher Scientific, Barcelona, Spain) and NucleoSpin® RNA Virus columns (Macherey-Nagel) according to manufacturer's instructions. Viral load for either 3249 strain or Lena strain was quantified by RT-qPCR using VetMAX™ PRRSV EU/NA 2.0 kit (Thermo Fisher Scientific, Barcelona, Spain). Amplifications were performed in duplicate from each animal in the QuantStudio 5 Real-time PCR System (Thermo Fisher Scientific) for 5 minutes (min) at 50 °C, 10 min at 95 °C followed by 40 cycles of 3 seconds (s) at 95 °C and 30 s at 60 °C. PRRSV RNA quantification was performed using specific primers of the target gene (Lena strain ORF7: forward primer AGCGCCAATTCAGAAAGAAA, reverse primer TGGATCGATTGCAGACAGAG; 3249 strain ORF7: forward primer GGCAAACGAGCTGTTAAACG, reverse primer AATTTCGGTCACATGGTTCC; Darwich et al., 2011). The ORF7 RT-PCR product from both 3249 and Lena strains was

201 firstly EtOH precipitated and purified using ExoSAP-ITTM (Thermo Fisher Scientific,
202 Barcelona, Spain). The purified products were quantified using BioDrop (BioDrop, UK).
203 Serial 10-fold dilutions of 3249 or Lena ORF7 RT-PCR products with known quantities,
204 ranging from 10^8 to 10^2 genomic copies/mL were used as standards to generate a standard
205 curve and, therefore, to determine the PRRSV genomic copies in sera and lung. The RT-
206 qPCR efficiency (E) was estimated for each strain by a linear regression model. The E
207 value was calculated from the slope of the standard curve according to equation:
208 $E=10^{(-1/slope)}-1$. Also, a set of eight serial 10-fold dilutions of know $TCID_{50}$/mL (starting
209 from 10^6 $TCID_{50}$/mL) was included in order to determine a relation between Ct-values,
210 genomic copies/mL and $TCID_{50}$/mL. An inter-run calibrator sample with a known
211 number of PRRSV copies was introduced in each experiment to self-control inter-run
212 variation. The area under the curve (AUC) for viremia and lung viral load was calculated
213 using the trapezoidal approach (Greenbaum et al., 2001). Results of viral load in sera and
214 lung are showed in equivalent $TCID_{50}$ (eq $TCID_{50}$) per mL.
215
216 *2.5. Antibody and serological assessments*
217 Specific antibodies against PRRSV were detected using IDEXX PRRS X3 ELISA test
218 (IDEXX laboratories, Barcelona, Spain) following manufacturer's instructions. Levels of
219 IFN-γ, IL-6 and IL-10 and the acute phase protein lipopolysaccharide binding protein
220 (LBP) as well as the soluble form of swine CD163 (sCD163) were assessed in sera from
221 all piglets. Different commercially available ELISA tests were used in accordance with
222 manufacturer's guidelines (IFN-γ, IL-6, IL-10 [Invitrogen, Barcelona, Spain]; LBP,
223 [Hycult Biotech, Uden, Netherlands]; sCD163 [Cusabio Biotech, Houston, USA]).
224 Results were expressed in pg/mL for IFN-γ, IL-6 and IL-10, and ng/mL for LBP and

sCD163. The minimum detectable concentrations were 2 pg/mL for IFN-γ, 45 pg/mL for IL-6, 3 pg/mL for IL-10, 1.6 ng/mL for LBP and 23.4 ng/mL for sCD163.

2.6. Immunohistochemistry in lung tissue

Four-micron sections from lung were dewaxed in xylene and rehydrated in descending grades of alcohol until distilled water. Then, endogenous peroxidase inhibition was performed in a 3% H_2O_2 solution in methanol for 30 min. Epitope demasking, primary antibodies dilutions and blocking of non-specific binding are detailed in Table 1. Monoclonal primary antibodies were incubated overnight at 4 ºC in a humid chamber. Polyclonal goat anti-mouse immunoglobulins (Agilent Technologies, Madrid, Spain) or polyclonal goat anti-rabbit immunoglobulins (Vector laboratories, USA) biotinylated secondary antibodies were accordingly incubated for 30 min at room temperature. After washing in PBS, Avidin–Biotin–Peroxidase complex technique (ABC Vector Elite, Vector laboratories, USA) was applied and the immunolabelling was revealed by application of NovaRED™ substrate kit (Vector Laboratories). Sections were counterstained with Harris's haematoxylin, dehydrated and mounted. PBS (pH 7.4) and Tris buffered saline (pH 7.6) were used as wash and diluent buffers, respectively. Antibody specificity was verified by exchanging the primary antibody by isotype matched reagents of irrelevant specificity. One negative control which consisted of replacement of the primary antibody by BSA blocking solution was included in each immunohistochemical assay to rule out non-specific bindings.

2.7. Immunohistochemistry cell counting

The number of immunolabelled cells was quantified in 25 non-overlapping selected high magnification fields of 0.2 mm^2 (Olympus BX51, Olympus Iberia SAU, L'Hospitalet de

Llobregat, Barcelona, Spain) and expressed as the mean of the score for each animal per mm^2. Labelled cells were morphologically identified by differentiating among PAMs, PIMs and interstitial macrophages.

2.8. Statistical analyses

Differences between groups were evaluated for approximate normality of distribution by the D'Agostino and Pearson omnibus normality test followed by the Mann Whitney's U non-parametric mean comparisons test. Correlation coefficients were assessed by the Spearman and Pearson tests and were considered relevant with $r > 0.6$ and $P < 0.05$. Data analyses and figures were performed by using GraphPad Prism 7.0 software (GraphPad Prism software 7.0, Inc., San Diego, CA, USA) and InkScape 0.92 software. A *P* value lower than 0.05 was considered statistically significant and represented as * $P \leq 0.05$, ** $P \leq 0.01$ *** $P \leq 0.001$ and **** $P \leq 0.0001$.

3. Results

3.1. Acute suppurative bronchopneumonia and the highest rectal temperature and clinical signs score were observed in Lena-infected pigs

Clinical observations and gross pathology of lung were described thoroughly by Rodríguez-Gómez et al. (2019). In brief, piglets inoculated with virulent Lena strain had a long period of hyperthermia (mean rectal temperature above 40.5 °C) with marked clinical signs score from 4 dpi onwards, both peaking at 6 dpi (Figs. 1A-1B, clinical signs score and temperature). By contrast, an increase in rectal temperature below the hyperthermic threshold accompanied by mild clinical signs was observed in piglets infected with 3249 strain (Figs. 1A-1B). At necropsy, tan-mottled areas, atelectasis, rubbery consistency, and consolidated areas were observed in the lungs from both

PRRSV-1-infected pigs whose macroscopic lung score gradually increased throughout the study (Figs. 1C-1D). In particular, a stronger and earlier onset of the lung lesion (from 6 dpi onwards) associated with the presence of extensive consolidated areas in apical and medial lobes as well as more severe interstitial pneumonia were observed in Lena-infected pigs causing the highest macroscopic lung score compared to 3249-infected pigs (Figs. 1C-1D).

A mild to moderate interstitial pneumonia with thickening of the alveolar septa by infiltrate of lymphocytes and macrophages was caused by both Lena and 3249 strains (Figs. 1E-1F). Furthermore, a suppurative bronchopneumonia characterised by neutrophils, cell debris and mucus filling the bronchial, bronchiolar and alveolar lumen was observed in lung section from Lena-infected pigs at 6 and 8 dpi (Figs. 1E-1F). A strong statistical correlation was found among temperature, clinical signs score, macroscopic and microscopic lung scores in Lena-infected pigs (Table 2).

3.2. Viraemia and lung viral load followed a similar kinetics in PRRSV-1-infected pigs

Viraemia and lung viral load were determined by RT-qPCR (efficiency of 99 %; slope = 3.34; detection limit: 1 copy/µl; slope-intercept = 39.5; and high linearity, r = 0.99). All animals were negative by RT-qPCR at day 0 and control pigs remained so all throughout the experiment. In sera, four out of five 3249-infected pigs and all Lena-infected pigs were PRRSV positive as early as 1 dpi. Viraemia was always higher in Lena- than in 3249-infected pigs from 1 to 8 dpi ($P < 0.01$ at 1, 3, 6 dpi; $P<0.05$ at 8 dpi), reaching the highest viral load at 6 dpi ($1.9x10^7$ eq $TCID_{50}$/mL). The AUC for viremia (mean) in Lena and 3249 group were 44.8 and 33.8 respectively (Fig. 2A). The viral load in the lung displayed a similar kinetics to that of serum for both infected groups, reaching the

maximum lung viral loads at 6 dpi in Lena group ($1.6x10^7$ eq $TCID_{50}$/mL), whereas 3249 group peaked at 8 dpi ($1.9x10^6$ eq $TCID_{50}$/mL) (Fig. 2B). By contrast to sera, PRRSV-1 was just detected in lung in two out of five animals in both infected groups at 1 dpi, being positive all infected piglets from 3 dpi onwards. The AUC for lung viral load (mean) in Lena group was 45 and 36.2 for 3249 group (Fig. 2B). In Lena infected-group the statistical analysis revealed a positive correlation among viraemia, lung viral load, temperature, clinical signs score and the number of PRRSV-N-protein$^+$ cells in the lungs (Table 2). A correlation among lung viral load and viraemia and PRRSV-N-protein$^+$ cells was also observed in 3249-infected pigs (r = 0.71, $P < 0.0001$; and, r = 0.60, $P < 0.005$, respectively).

3.3. A significant increase in the serum concentration of IFN-γ was observed in Lena-infected pigs when compared with 3249-infected pigs

PRRSV-specific antibodies were first detected at 8 dpi in sera from both PRRSV-1-infected groups (non-significant differences in S/P ratios) (data not shown). A significant increase in IFN-γ serum levels was detected after Lena infection at 6 and 8 dpi (maximum mean level of 234 ± 100 pg/mL at 6 dpi) compared to control ($P<0.05$) and 3249 ($P<0.01$) groups (Fig. 2C). Maximum IL-6 levels in serum of 3249 group were observed at 6 dpi (mean of 350 ± 220 pg/mL), whereas pigs belonging to Lena group reached the highest IL-6 levels at 8 dpi (mean of 480 ± 50 pg/mL) (Fig. 2D). IL-10, LBP or sCD163 were not detected in serum samples from both control and infected groups throughout the study. Both viraemia and lung viral load displayed a positive statistical correlation with IFN-γ levels, which in turn were also correlated with temperature and the clinical signs score in Lena infected-pigs (Table 2).

3.4. The increase in the number of PRRSV-N-protein$^+$ cells was associated with a decrease of CD163$^+$ macrophages in the lung of PRRSV-infected pigs

The labelling of PRRSV-N-protein was mainly observed in PAMs and in a lesser extent in interstitial and intravascular macrophages (Figs. 3A-3B). In Lena-infected pigs, clusters of PRRSV-N-protein$^+$ macrophages were observed within foci of bronchopneumonia at 6 and 8 dpi (Fig. 3B inset). A progressive increase in the number of PRRSV-N-protein$^+$ cells was detected throughout the study in both PRRSV-1-infected groups, reaching a peak at 6 and 8 dpi in Lena and 3249-infected piglets, respectively. This increase was significantly higher in Lena than in 3249 group (P<0.05 at 3, 6 and 8 dpi) (Fig. 3E, primary axis). No positive cells were detected in control pigs.

CD163 immunolabelling was detected in the cell membrane and cytoplasm of PAMs, interstitial macrophages and, occasionally, intravascular macrophages (Figs. 3C-3D, insets). A drop in the number of CD163$^+$ cells was observed from 3 to 8 dpi in both PRRSV-1-infected groups. This decrease was more intense in Lena-infected animals when compared to 3249 (P<0.05 at 3 dpi) and control groups (P<0.05 at 3 and 8 dpi) (Fig. 3E, secondary axis). By contrast, the frequency of CD163$^+$ cells remained constant in control pigs during the whole study. Of note, PAMs were the subset of pulmonary macrophages which underwent the strongest reduction in the number of CD163$^+$ cells. Furthermore, the frequency of CD163$^+$ cells showed a strong negative correlation with lung viral load and the number of PRRSV-N-protein$^+$ cells in Lena infected-pigs (Fig. 3E) (Table 2).

3.5. A strong influx of CD14$^+$ macrophages and monocytes infiltrating the interstitium was detected in Lena-infected pigs

The labelling against CD14 was mainly observed in the cell membrane and cytoplasm of monocytes, interstitial and intravascular macrophages and, occasionally, in PAMs (Figs. 4A-4B, insets). Whereas no changes were observed in the number of $CD14^+$ cells in the control group along the study, a gradual increase with maximum expression at 8 dpi was detected in both infected groups (Fig. 4E). Lena-infected pigs showed the highest frequency of $CD14^+$ cells when compared to control animals ($P<0.01$) in association with the presence of suppurative bronchopneumonia (Fig. 4B). $CD14^+$ interstitial and intravascular macrophages were observed infiltrating extensive areas of the interstitium, whereas almost no $CD14^+$ cells were present in the bronchial wall and alveolar lumen. Interestingly, the number of $CD14^+$ cells in Lena-infected piglets displayed a strong positive correlation with the concentration of IL-6 in sera (Table 2).

3.6. Lena virulent strain induced a strong increase of $iNOS^+$ cells associated with a higher microscopic lung lesion

The granular intracytoplasmic immunostaining of iNOS was primarily observed in PAMs and interstitial macrophages in foci of interstitial pneumonia and bronchopneumonia (Figs. 4C-4D). The number of $iNOS^+$ cells followed a similar kinetics in both PRRSV-1-infected groups, with a progressive increase from 6 dpi onwards, reaching a significant increase by the end of the study (8 dpi) in Lena-infected pigs compared to 3249 ($P<0.01$) and control groups ($P<0.05$) (Fig. 4F).

3.7. The increase of $CD200R1^+$ cells along the study was highly correlated with the course of lung injury

CD200R1 labelling was detected in the cytoplasm of intravascular and interstitial macrophages located inside or surrounding bronchopneumonia foci, with occasional

expression in PAMs and monocytes (Figs. 5A-5B, insets). Whereas the number of CD200R1$^+$ cells significantly increased in Lena-infected pigs at 6-8 dpi (P<0.05 at 6 dpi with respect to 3249 group; and P<0.01 at 6 dpi and P<0.05 at 8 dpi with respect to control group), this increase was just detected at 8 dpi in 3249-infected pigs (P<0.05 with respect to control group) (Fig. 5E, primary axis). Control animals presented a scarce number of CD200R1$^+$ cells along the study. For Lena infected-pigs a strong positive correlation was observed among the frequency of CD200R1$^+$ cells and the microscopic lung lesions (Fig. 5E) (Table 2).

3.8. Both PRRSV-1 strains induced an increase of FoxP3$^+$ cells at 6-8 dpi.

FoxP3 yielded a nuclear immunolabelling in lymphocytes mainly located in areas of atelectasis and interstitial pneumonia (Figs. 5C-5D, insets). Although two Lena-infected pigs exhibited a higher number of FoxP3$^+$ cells at 1 dpi, the kinetics of positive cells for this immune markers showed a gradual increase along the study in both Lena- and 3249-infected animals, reaching the maximum at 6 dpi (Fig. 5F). There were no significant differences in the number of FoxpP3$^+$ cells among infected groups. However, a significant increase of FoxP3$^+$ cells was detected at 6 and 8 dpi in Lena-infected pigs compared to control animals (P<0.05).

Discussion

PRRSV plays a pivotal role in PRDC, modulating the host immune response and favouring secondary bacterial infections (Gómez-Laguna et al., 2013; Van Gucht et al., 2004). Virulent PRRSV-1 strains cause more severe clinical signs, higher mortality rates as well as marked lung injury with a higher incidence of bronchopneumonia as opposed to low virulent strains (Amarilla et al., 2015; Canelli et al., 2017; Frydas et al., 2013;

Gómez-Laguna et al., 2010; Morgan et al., 2013; Renson et al., 2017; Rodríguez-Gómez et al., 2019; Stadejek et al., 2017; Weesendorp et al., 2013). Accordingly, we hypothesise that severe pulmonary lesions observed along infection with virulent PRRSV-1 strains might be associated with a higher decrease in the amount of PAMs as well as an imbalance between anti- and pro-inflammatory responses with different molecules potentially involved in this process.

As previously described (Renson et al., 2017; Weesendorp et al., 2013), severe systemic and respiratory symptoms as well as hyperthermia were observed in animals infected with virulent Lena strain, whereas low virulent 3249 strain only caused mild clinical signs and a slightly increase of rectal temperature. Furthermore, virulent Lena strain caused an earlier and stronger onset of lung lesions due to extensive consolidated areas in the apical and medial lobes which were microscopically linked to suppurative bronchopneumonia as well as severe characteristic interstitial pneumonia. On the other hand, PRRSV virulence has been associated with higher virus titre and antibody response *in vivo* (Brockmeier et al., 2012; Lu et al., 2014) Although Lena virulent strain elicited a quite higher viraemia than the low virulent strain, no differences were observed in the antibody response in the early phase of infection. Similar results have been previously reported by others when comparing Lena with low virulent strains (Renson et al., 2017; Weesendorp et al., 2013), and confirm that PRRSV-1 virulence and specific non-neutralizing antibodies are not associated in the acute phase of infection.

PRRSV infection with virulent strains usually induces a strong inflammatory immune response when compared with low virulent strains (Amarilla et al., 2015; Liu et al., 2010; Morgan et al., 2013; Renson et al., 2017; Weesendorp et al., 2013). In our study, higher

levels of IL-6 at 8 dpi and IFN-γ at 6-8 dpi were detected in the sera of Lena-infected pigs. Increased concentration of IL-6 in plasma is associated with both systemic and respiratory symptoms (Van Reeth and Nauwynck, 2000) and could play a dual role during virus infection: (i) protecting the host from infection and (ii) inducing inflammation and tissue damage when it is overexpressed (Liu et al., 2010). It is known that IFN-γ is, mostly produced by activated NK cells, NKT cells, γ/δ T cells, cytotoxic T cells and memory T cells (Gerner et al., 2015; Mair et al., 2014), and participates in regulating the immune and inflammatory responses (Van Reeth and Nauwynck, 2000). In fact, an early increase of NKT cells has been associated with viraemia peak in piglets infected with PR40 virulent strain (Ferrari et al., 2018). In our study, virulent Lena strain elicited a marked increase in the serum level of IFN-γ which was significantly correlated with viremia and lung viral load, suggesting an attempt of the host innate immune response in controlling virus replication. The enhanced serum concentration of IL-6 could mirror the stronger systemic inflammatory response induced by Lena during the acute phase response contributing to the fever and more severe clinical signs as well as lung lesion that specifically arise in virulent PRRSV-1 strains (Amarilla et al., 2015; Renson et al., 2017).

In order to evaluate the kinetics of PRRSV-1 in the lung, we analysed the expression of PRRSV-N-protein and lung viral load. Interestingly, both the number of PRRSV-N-protein$^+$ cells and lung viral load showed a solid negative correlation with the frequency of CD163$^+$ cells, the essential host receptor for PRRSV infection (Burkard et al., 2017; Van Gorp et al., 2008; Whitworth et al., 2016). The dramatical depletion in the frequency of pulmonary CD163$^+$ cells in Lena-infected animals has been already reported in live PAMs from the BALF of Lena-infected piglets (Renson et al., 2017; Rodríguez-Gómez et al., 2019) as well as from lung tissue sections of piglets infected with virulent SU1-bel

strain (Sánchez-Carvajal et al., 2019). This finding could be due to the direct cytopathic effect of the virus in its target cell but also to an indirect induction of regulated cell death in infected and non-infected cells, which has been broadly described in the lung and lymphoid organs of pigs infected with virulent PRRSV-1 strains (Morgan et al., 2013; Ruedas-Torres et al., 2020; Sánchez-Carvajal et al., 2019). Another possibility would be the shedding of sCD163 due to macrophages activation either by a direct effect of the virus or secondary to viral infection (Møller, 2012). However, it seems unlikely, since no changes were detected in sCD163 sera concentration in our study after infection with a virulent PRRSV-1 strain. In contrast, *Glaesserella parasuis* virulent strains have been reported to increase serum levels of sCD163 linked to a reduction in CD163 surface expression in PAMs (Costa-Hurtado et al., 2013). In our study, the decrease of $CD163^+$ macrophages, an important cell subset to tackle bacterial infections (Fabriek et al., 2009), points out to a mechanism involved in the impairment of the local pulmonary immune response. This fact may potentially favour the co-infection with secondary commensal microorganisms leading to bronchopneumonia.

CD14 and iNOS are involved in lung inflammation after infection with PRRSV (Chen et al., 2014; Lee and Kleiboeker, 2005; Van Gucht et al., 2004, 2005; Yan et al., 2017) Upregulation of CD14, as lipopolysaccharides (LPS) co-receptor, after infection with PRRSV sensitises the lungs for the production of proinflammatory cytokines and respiratory signs upon exposure to bacterial LPS (Van Gucht et al., 2005). For its part, iNOS is mainly expressed in response to different stimuli, such as cytokines and LPS, playing a role in tissue injury upon production of NO (Chen et al., 2014; Cho and Chae, 2002; Vlahos et al., 2011; Yan et al., 2017). In this study, an increase in the number of $CD14^+$ cells after PRRSV-1 infection was observed in association with suppurative

475 bronchopneumonia, which was more evident in Lena-infected piglets at 6 – 8 dpi. This
476 increase was mainly due to $CD14^+$ monocytes, interstitial and intravascular macrophages
477 infiltrating extensive areas of the interstitium. The influx of $CD14^+$ monocytes and
478 immature macrophages may be explained by an attempt to replenish the loss of $CD163^+$
479 macrophages contributing to clearance of cellular debris and resolution of inflammation,
480 restoring the normal lung function. On the other hand, the increase of $CD14^+$ cells implies
481 a higher availability of the LPS-LBP complex receptor, which is likely to sensitise the
482 lung to future secondary bacterial infections making the onset of PRDC easier (Van Gucht
483 et al., 2005). In the case of iNOS, a significant increase in the number of $iNOS^+$ cells was
484 observed in areas of interstitial pneumonia as well as bronchopneumonia in Lena-infected
485 pigs. The induction of iNOS has been associated with both a direct effect of the viral
486 replication or viral components and an indirect effect mediated by cytokines, such as IFN-
487 γ, or by LPS (Akaike and Maeda, 2000; Chen et al., 2014; Lee and Kleiboeker, 2005). Of
488 note, the peak of iNOS in Lena-infected animals appeared in our study just after the peak
489 of PRRSV replication in the lung as well as after the peak of serum IFN-γ, being
490 associated with the maximum lung injury and bronchopneumonia lesion. These factors
491 may play a role in the regulation of iNOS expression along PRRSV infection and its role
492 in lung injury development (Chen et al., 2014; Lee and Kleiboeker, 2005; Yan et al.,
493 2017).
494
495 After a cascade of proinflammatory events, the host is able to trigger off the release of
496 anti-inflammatory or regulatory mediators to restrain the extent of the injury. Thus, the
497 role of CD200R1 and FoxP3 was evaluated in the present study. A strong positive
498 correlation was detected among the frequency of $CD200R1^+$ cells and the microscopic
499 score which was mainly associated with a higher severity of typical interstitial pneumonia

and suppurative bronchopneumonia in Lena-infected pigs. Likewise, an increase in the frequency of $FoxP3^+$ cells between 6 and 8 dpi was triggered by both PRRSV-1 strains when the lung injury was higher. CD200R1 has been involved in reducing the expression of pro-inflammatory cytokines in a wide range of inflammatory diseases (Vaine and Soberman, 2014), nevertheless to the best of the authors' knowledge, the role of CD200R1 in viral diseases of swine is largely unknown. Previous studies in a murine model reported that influenza virus infection induced the upregulation of CD200R1 in macrophages, decreasing their responsiveness and increasing the sensitivity to bacterial infection and finally severe lung injury (Snelgrove et al., 2008; Vaine and Soberman, 2014). In contrast, CD200/CD200R1 signalling pathway limited type I IFN production during coronavirus infection protecting the host from cytokine storm (Vaine and Soberman, 2014). In addition, FoxP3 has been reported as a potential inhibitor of the cell-mediated immune response in pigs upon PRRSV infection (Ferrarini et al., 2015; Silva-Campa et al., 2009; 2010); but also induction of Tregs has been described in the lungs and tracheobronchial lymph nodes in PRRSV-infected pigs (Nedumpun et al., 2018). However, its role in the immunopathogenesis of PRRSV-induced lung injury is unexplored. PD1/PDL1 modulation and $FoxP3^+$ cells have been pointed out to play a dual role upon viral infections, restricting immune inflammation-induced tissue damage and encouraging lung repair during acute phase of infection (Lin et al., 2018; Singh et al., 2019), but leading to exhaustion and suppression of antiviral immune responses in the chronic infection (Arpaia et al., 2015; Schönrich and Raftery, 2019; Wang et al., 2018). Taken together, our results highlight the upregulation of CD200R1 and FoxP3 as mechanisms involved in the constraint and recovery of lung injury during acute PRRSV infection. Further studies are needed to determine the mechanisms involved in the

activation of these molecules during acute PRRSV as well as their role and related signalling pathways along the persistent infection.

5. Conclusion

The present study dissects the immunopathology of lung injury along an acute infection with PRRSV-1 strains of different virulence, revealing a drop in the number of $CD163^+$ cells together with an enhancement in the expression of CD14 and iNOS as mechanisms involved in the earlier and higher extent of lung lesion in Lena-infected piglets. These changes could sensitise the lung to future secondary bacterial infections. In addition, the increase in the number of $CD14^+$ cells is likely to respond to an attempt to replenish the $CD163^+$ macrophages subset lost along the infection with both PRRSV-1 strains. On the other hand, the increase in the expression of CD200R1 and FoxP3 represents potential pathways activated to contain the inflammatory response.

Conflict of interest

The authors declare that they have no competing interest.

Acknowledgements

We express our appreciation to Gema Muñoz, Alberto Alcántara and Esmeralda Cano for their technical assistance and Dr. Hans Nauwynck for providing us the PRRSV-1 subtype 3 Lena strain. This work was supported by the Spanish Ministry of Economy and Competitiveness (AGL2016-76111-R). J. Gómez-Laguna is supported by a "Ramón y Cajal" contract of the Spanish Ministry of Economy and Competitiveness (RyC-2014-16735).

549 **References**

550 Amarilla, S. P., Gómez-Laguna, J., Carrasco, L., Rodríguez-Gómez, I. M., Caridad y
551 Ocerín, J. M., Morgan, S. B., Graham, S. P., Frossard, J. P., Drew, T. W., &
552 Salguero, F. J. (2015). A comparative study of the local cytokine response in the
553 lungs of pigs experimentally infected with different PRRSV-1 strains:
554 Upregulation of IL-1α in highly pathogenic strain induced lesions. *Veterinary*
555 *Immunology and Immunopathology*, *164*(3–4), 137–147.
556 https://doi.org/10.1016/j.vetimm.2015.02.003

557 Arpaia, N., Green, J. A., Moltedo, B., Arvey, A., Hemmers, S., Yuan, S., Treuting, P.
558 M., & Rudensky, A. Y. (2015). A Distinct Function of Regulatory T Cells in
559 Tissue Protection. *Cell*, *162*(5), 1078–1089.
560 https://doi.org/10.1016/j.cell.2015.08.021

561 Balka, G., Podgórska, K., Brar, M. S., Bálint, Á., Cadar, D., Celer, V., Dénes, L.,
562 Dirbakova, Z., Jedryczko, A., Márton, L., Novosel, D., Petrović, T., Sirakov, I.,
563 Szalay, D., Toplak, I., Leung, F. C. C., & Stadejek, T. (2018). Genetic diversity of
564 PRRSV 1 in Central Eastern Europe in 1994-2014: Origin and evolution of the
565 virus in the region. *Scientific Reports*, *8*(1), 1–12. https://doi.org/10.1038/s41598-
566 018-26036-w

567 Bordet, E., Maisonnasse, P., Renson, P., Bouguyon, E., Crisci, E., Tiret, M., Descamps,
568 D., Bernelin-Cottet, C., Urien, C., Lefèvre, F., Jouneau, L., Bourry, O., Leplat, J.
569 J., Schwartz-Cornil, I., & Bertho, N. (2018). Porcine alveolar macrophage-like
570 cells are pro-inflammatory pulmonary intravascular macrophages that produce
571 large titers of porcine reproductive and respiratory syndrome virus. *Scientific*
572 *Reports*, *8*(1), 10172. https://doi.org/10.1038/s41598-018-28234-y

573 Brockmeier, S. L., Loving, C. L., Nelson, E. A., Miller, L. C., Nicholson, T. L.,

574 Register, K. B., Grubman, M. J., Brough, D. E., & Kehrli, M. E. (2012). The
575 presence of alpha interferon at the time of infection alters the innate and adaptive
576 immune responses to porcine reproductive and respiratory syndrome virus.
577 *Clinical and Vaccine Immunology*, *19*(4), 508–514.
578 https://doi.org/10.1128/CVI.05490-11
579 Brockmeier, S. L., Loving, C. L., Palmer, M. V., Spear, A., Nicholson, T. L., Faaberg,
580 K. S., & Lager, K. M. (2017). Comparison of Asian porcine high fever disease
581 isolates of porcine reproductive and respiratory syndrome virus to United States
582 isolates for their ability to cause disease and secondary bacterial infection in swine.
583 *Veterinary Microbiology*, *203*, 6–17. https://doi.org/10.1016/j.vetmic.2017.02.003
584 Burkard, C., Lillico, S. G., Reid, E., Jackson, B., Mileham, A. J., Ait-Ali, T., Whitelaw,
585 C. B. A., & Archibald, A. L. (2017). Precision engineering for PRRSV resistance
586 in pigs: Macrophages from genome edited pigs lacking CD163 SRCR5 domain are
587 fully resistant to both PRRSV genotypes while maintaining biological function.
588 *PLoS Pathogens*, *13*(2), e1006206. https://doi.org/10.1371/journal.ppat.1006206
589 Canelli, E., Catella, A., Borghetti, P., Ferrari, L., Ogno, G., De Angelis, E., Corradi, A.,
590 Passeri, B., Bertani, V., Sandri, G., Bonilauri, P., Leung, F. C., Guazzetti, S., &
591 Martelli, P. (2017). Phenotypic characterization of a highly pathogenic Italian
592 porcine reproductive and respiratory syndrome virus (PRRSV) type 1 subtype 1
593 isolate in experimentally infected pigs. *Veterinary Microbiology*, *210*(July), 124–
594 133. https://doi.org/10.1016/j.vetmic.2017.09.002
595 Chen, X. xin, Quan, R., Guo, X. kun, Gao, L., Shi, J., & Feng, W. hai. (2014). Up-
596 regulation of pro-inflammatory factors by HP-PRRSV infection in microglia:
597 Implications for HP-PRRSV neuropathogenesis. *Veterinary Microbiology*, *170*(1–
598 2), 48–57. https://doi.org/10.1016/j.vetmic.2014.01.031

599 Cho, W. S., & Chae, C. (2002). Immunohistochemical detection and distribution of
600 inducible nitric oxide synthase in pigs naturally infected with Actinobacillus
601 pleuropneumoniae. *Journal of Comparative Pathology*, *126*(2–3), 109–114.
602 https://doi.org/10.1053/jcpa.2001.0529
603 Costa-Hurtado, M., Olvera, A., Martinez-Moliner, V., Galofré-Milà, N., Martínez, P.,
604 Dominguez, J., & Aragon, V. (2013). Changes in macrophage phenotype after
605 infection of pigs with haemophilus parasuis strains with different levels of
606 virulence. *Infection and Immunity*, *81*(7), 2327–2333.
607 https://doi.org/10.1128/IAI.00056-13
608 Darwich, L., Gimeno, M., Sibila, M., Diaz, I., de la Torre, E., Dotti, S., Kuzemtseva, L.,
609 Martin, M., Pujols, J., & Mateu, E. (2011). Genetic and immunobiological diversities
610 of porcine reproductive and respiratory syndrome genotype I strains. *Veterinary*
611 *Microbiology*, *150*(1–2), 49–62. https://doi.org/10.1016/j.vetmic.2011.01.008
612 Das, P. B., Dinh, P. X., Ansari, I. H., De Lima, M., Osorio, F. A., & Pattnaik, A. K.
613 (2010). The Minor Envelope Glycoproteins GP2a and GP4 of Porcine
614 Reproductive and Respiratory Syndrome Virus Interact with the Receptor CD163.
615 *Journal of Virology*, *84*(4), 1731–1740. https://doi.org/10.1128/JVI.01774-09
616 Duan, X., Nauwynck, H. J., & Pensaert, M. B. (1997). Virus quantification and
617 identification of cellular targets in the lungs and lymphoid tissues of pigs at
618 different time intervals after inoculation with porcine reproductive and respiratory
619 syndrome virus (PRRSV). *Veterinary Microbiology*, *56*(1–2), 9–19.
620 https://doi.org/10.1016/S0378-1135(96)01347-8
621 Elmore, M. R. P., Burton, M. D., Conrad, M. S., Rytych, J. L., Van Alstine, W. G., &
622 Johnson, R. W. (2014). Respiratory viral infection in neonatal piglets causes
623 marked microglia activation in the hippocampus and deficits in spatial learning.

Journal of Neuroscience, *34*(6), 2120–2129. https://doi.org/10.1523/JNEUROSCI.2180-13.2014

Fabriek, B. O., Bruggen, R. Van, Deng, D. M., Ligtenberg, A. J. M., Nazmi, K., Schornagel, K., Vloet, R. P. M., Dijkstra, C. D., & Van Den Berg, T. K. (2009). The macrophage scavenger receptor CD163 functions as an innate immune sensor for bacteria. *Blood*, *113*(4), 887–892. https://doi.org/10.1182/blood-2008-07-167064

Ferrari, L., Canelli, E., De Angelis, E., Catella, A., Ferrarini, G., Ogno, G., Bonati, L., Nardini, R., Borghetti, P., & Martelli, P. (2018). A highly pathogenic porcine reproductive and respiratory syndrome virus type 1 (PRRSV-1) strongly modulates cellular innate and adaptive immune subsets upon experimental infection. *Veterinary Microbiology*, *216*, 85–92. https://doi.org/10.1016/j.vetmic.2018.02.001

Ferrarini, G., Borghetti, P., De Angelis, E., Ferrari, L., Canelli, E., Catella, A., Di Lecce, R., & Martelli, P. (2015). Immunoregulatory signal FoxP3, cytokine gene expression and IFN-γ cell responsiveness upon porcine reproductive and respiratory syndrome virus (PRRSV) natural infection. *Research in Veterinary Science*, *103*, 96–102. https://doi.org/10.1016/j.rvsc.2015.09.018

Frydas, I. S., Verbeeck, M., Cao, J., & Nauwynck, H. J. (2013). Replication characteristics of porcine reproductive and respiratory syndrome virus (PRRSV) European subtype 1 (Lelystad) and subtype 3 (Lena) strains in nasal mucosa and cells of the monocytic lineage: Indications for the use of new receptors of PRRSV (Lena). *Veterinary Research*, *44*(1), 73. https://doi.org/10.1186/1297-9716-44-73

Geldhof, M. F., Vanhee, M., Van Breedam, W., Van Doorsselaere, J., Karniychuk, U. U., & Nauwynck, H. J. (2012). Comparison of the efficacy of autogenous inactivated Porcine Reproductive and Respiratory Syndrome Virus (PRRSV)

649 vaccines with that of commercial vaccines against homologous and heterologous
650 challenges. *BMC Veterinary Research*, *8*(1), 182. https://doi.org/10.1186/1746-
651 6148-8-182
652 Gerner, W., Talker, S. C., Koinig, H. C., Sedlak, C., Mair, K. H., & Saalmüller, A.
653 (2015). Phenotypic and functional differentiation of porcine αβ T cells: Current
654 knowledge and available tools. *Molecular Immunology*, *66*(1), 3–13.
655 https://doi.org/10.1016/j.molimm.2014.10.025
656 Gimeno, M., Darwich, L., Diaz, I., De La Torre, E., Pujols, J., Martín, M., Inumaru, S.,
657 Cano, E., Domingo, M., Montoya, M., & Mateu, E. (2011). Cytokine profiles and
658 phenotype regulation of antigen presenting cells by genotype-I porcine
659 reproductive and respiratory syndrome virus isolates. *Veterinary Research*, *42*(1),
660 9. https://doi.org/10.1186/1297-9716-42-9
661 Gómez-Laguna, J., Salguero, F. J., Barranco, I., Pallarés, F. J., Rodríguez-Gómez, I. M.,
662 Bernabé, A., & Carrasco, L. (2010). Cytokine Expression by Macrophages in the
663 Lung of Pigs Infected with the Porcine Reproductive and Respiratory Syndrome
664 Virus. *Journal of Comparative Pathology*, *142*(1), 51–60.
665 https://doi.org/10.1016/j.jcpa.2009.07.004
666 Gómez-Laguna, J., Salguero, F. J., Pallarés, F. J., & Carrasco, L. (2013).
667 Immunopathogenesis of porcine reproductive and respiratory syndrome in the
668 respiratory tract of pigs. *The Veterinary Journal*, *195*(2), 148–155.
669 https://doi.org/10.1016/j.tvjl.2012.11.012
670 Gorbalenya AE, Krupovic M, Siddell S, Varsani A, K. J. (2018). *International*
671 *Committee on Taxonomy of Viruses (ICTV)*. Retrieved 6 April 2019, from
672 International Committee on Taxonomy of Viruses (ICTV) Website:
673 Https://Talk.Ictvonline.Org/Taxonomy/p/Taxonomy-

History?Taxnode_id=20186087. https://talk.ictvonline.org/taxonomy/p/taxonomy-history?taxnode_id=20186087

Greenbaum, E., Furst, A., Kiderman, A., Stewart, B., Levy, R., Schlesinger, M., Morag, A., & Zakay-Rones, Z. (2001). Area under the viraemia curve versus absolute viral load: Utility for predicting symptomatic cytomegalovirus infections in kidney transplant patients. *Journal of Medical Virology*, *65*(1), 85–89. https://doi.org/10.1002/jmv.2005

Halbur, P. G., Paul, P. S., Meng, X. J., Lum, M. A., Andrews, J. J., & Rathje, J. A. (1996). Comparative pathogenicity of nine US porcine reproductive and respiratory syndrome virus (PRRSV) isolates in a five-week-old cesarean-derived, colostrum-deprived pig model. *Journal of Veterinary Diagnostic Investigation*, *8*(1), 11–20. https://doi.org/10.1177/104063879600800103

Karniychuk, U. U., Geldhof, M., Vanhee, M., Van Doorsselaere, J., Saveleva, T. A., & Nauwynck, H. J. (2010). Pathogenesis and antigenic characterization of a new East European subtype 3 porcine reproductive and respiratory syndrome virus isolate. *BMC Veterinary Research*, *6*(1), 30. https://doi.org/10.1186/1746-6148-6-30

Käser, T., Gerner, W., Hammer, S. E., Patzl, M., & Saalmüller, A. (2008). Detection of Foxp3 protein expression in porcine T lymphocytes. *Veterinary Immunology and Immunopathology*, *125*(1–2), 92–101. https://doi.org/10.1016/j.vetimm.2008.05.007

Lee, S. M., & Kleiboeker, S. B. (2005). Porcine arterivirus activates the NF-κB pathway through IκB degradation. *Virology*, *342*(1), 47–59. https://doi.org/10.1016/j.virol.2005.07.034

Lin, S., Wu, H., Wang, C., Xiao, Z., & Xu, F. (2018). Regulatory T cells and acute lung injury: Cytokines, uncontrolled inflammation, and therapeutic implications. In

699 *Frontiers in Immunology* (Vol. 9, Issue JUL). Frontiers Media S.A.
700 https://doi.org/10.3389/fimmu.2018.01545
701 Liu, Y., Shi, W., Zhou, E., Wang, S., Hu, S., Cai, X., Rong, F., Wu, J., Xu, M., Xu, M.,
702 & Li, Q. (2010). Dynamic changes in inflammatory cytokines in pigs infected with
703 highly pathogenic porcine reproductive and respiratory syndrome virus. *Clinical*
704 *and Vaccine Immunology*, *17*(9), 1439–1445. https://doi.org/10.1128/CVI.00517-
705 09
706 Lu, W., Sun, B., Mo, J., Zeng, X., Zhang, G., Wang, L., Zhou, Q., Zhu, L., Li, Z., Xie,
707 Q., Bi, Y., & Ma, J. (2014). Attenuation and Immunogenicity of a Live High
708 Pathogenic PRRSV Vaccine Candidate with a 32-Amino Acid Deletion in the nsp2
709 Protein. *Journal of Immunology Research*, *2014*, 1–11.
710 https://doi.org/10.1155/2014/810523
711 Lunney, J. K., Fritz, E. R., Reecy, J. M., Kuhar, D., Prucnal, E., Molina, R.,
712 Christopher-Hennings, J., Zimmerman, J., & Rowland, R. R. R. (2010).
713 Interleukin-8, interleukin-1beta, and interferon-gamma levels are linked to PRRS
714 virus clearance. *Viral Immunology*, *23*(2), 127–134.
715 https://doi.org/10.1089/vim.2009.0087
716 Mair, K. H., Sedlak, C., Käser, T., Pasternak, A., Levast, B., Gerner, W., Saalmüller,
717 A., Summerfield, A., Gerdts, V., Wilson, H. L., & Meurens, F. (2014). The porcine
718 innate immune system: An update. In *Developmental and Comparative*
719 *Immunology* (Vol. 45, Issue 2, pp. 321–343). Elsevier Ltd.
720 https://doi.org/10.1016/j.dci.2014.03.022
721 Mattsson, J. G., Bergström, K., Wallgren, P., & Johansson, K.-E. E. (1995). Detection
722 of Mycoplasma hyopneumoniae in nose swabs from pigs by in vitro amplification
723 of the 16S rRNA gene. *Journal of Clinical Microbiology*, *33*(4), 893–897.

http://www.ncbi.nlm.nih.gov/pubmed/7540629

Møller, H. J. (2012). Soluble CD163. *Scandinavian Journal of Clinical and Laboratory Investigation*, *163*(1), 1–13. https://doi.org/10.3109/00365513.2011.626868

Morgan, S. B., Frossard, J. P., Pallares, F. J., Gough, J., Stadejek, T., Graham, S. P., Steinbach, F., Drew, T. W., & Salguero, F. J. (2016). Pathology and Virus Distribution in the Lung and Lymphoid Tissues of Pigs Experimentally Inoculated with Three Distinct Type 1 PRRS Virus Isolates of Varying Pathogenicity. *Transboundary and Emerging Diseases*, *63*(3), 285–295. https://doi.org/10.1111/tbed.12272

Morgan, S. B., Graham, S. P., Salguero, F. J., Sánchez Cordón, P. J., Mokhtar, H., Rebel, J. M. J., Weesendorp, E., Bodman-Smith, K. B., Steinbach, F., & Frossard, J. P. (2013). Increased pathogenicity of European porcine reproductive and respiratory syndrome virus is associated with enhanced adaptive responses and viral clearance. *Veterinary Microbiology*, *163*(1–2), 13–22. https://doi.org/10.1016/j.vetmic.2012.11.024

Nedumpun, T., Sirisereewan, C., Thanmuan, C., Techapongtada, P., Puntarotairung, R., Naraprasertkul, S., Thanawongnuwech, R., & Suradhat, S. (2018). Induction of porcine reproductive and respiratory syndrome virus (PRRSV)-specific regulatory T lymphocytes (Treg) in the lungs and tracheobronchial lymph nodes of PRRSV-infected pigs. *Veterinary Microbiology*, *216*, 13–19. https://doi.org/10.1016/j.vetmic.2018.01.014

Ogno, G., Rodríguez-Gómez, I. M., Canelli, E., Ruedas-Torres, I., Álvarez, B., Domínguez, J., Borghetti, P., Martelli, P., & Gómez-Laguna, J. (2019). Impact of PRRSV strains of different in vivo virulence on the macrophage population of the thymus. *Veterinary Microbiology*, *232*, 137–145.

https://doi.org/10.1016/j.vetmic.2019.04.016

Pasternak, J. A., MacPhee, D. J., & Harding, J. C. S. (2019). Development and application of a porcine specific ELISA for the quantification of soluble CD163. *Veterinary Immunology and Immunopathology*, *210*, 60–67. https://doi.org/10.1016/j.vetimm.2019.03.011

Poderoso, T., Martínez de la Riva, P., Uenishi, H., Alvarez, B., Toki, D., Nieto-Pelegrín, E., Alonso, F., Domínguez, J., Ezquerra, A., & Revilla, C. (2019). Analysis of the expression of porcine CD200R1 and CD200R1L by using newly developed monoclonal antibodies. *Developmental & Comparative Immunology*, *100*(June), 103417. https://doi.org/10.1016/j.dci.2019.103417

Renson, P., Rose, N., Le Dimna, M., Mahé, S., Keranflec'h, A., Paboeuf, F., Belloc, C., Le Potier, M. F., & Bourry, O. (2017). Dynamic changes in bronchoalveolar macrophages and cytokines during infection of pigs with a highly or low pathogenic genotype 1 PRRSV strain. *Veterinary Research*, *48*(1), 15. https://doi.org/10.1186/s13567-017-0420-y

Rodríguez-Gómez, I. M., Gómez-Laguna, J., Barranco, I., Pallarés, F. J., Ramis, G., Salguero, F. J., & Carrasco, L. (2013). Downregulation of antigen-presenting cells in tonsil and lymph nodes of porcine reproductive and respiratory syndrome virus-infected pigs. *Transboundary and Emerging Diseases*, *60*(5), 425–437. https://doi.org/10.1111/j.1865-1682.2012.01363.x

Rodríguez-Gómez, Irene M., Sánchez-Carvajal, J. M., Pallarés, F. J., Mateu, E., Carrasco, L., & Gómez-Laguna, J. (2019). Virulent Lena strain induced an earlier and stronger downregulation of CD163 in bronchoalveolar lavage cells. *Veterinary Microbiology*, *235*, 101–109. https://doi.org/10.1016/j.vetmic.2019.06.011

Rowland, R. R. R., Steffen, M., Ackerman, T., & Benfield, D. A. (1999). The evolution

of porcine reproductive and respiratory syndrome virus: Quasispecies and emergence of a virus subpopulation during infection of pigs with VR-2332. *Virology*, *259*(2), 262–266. https://doi.org/10.1006/viro.1999.9789

Ruedas-Torres, I., Rodríguez-Gómez, I. M., Sánchez-Carvajal, J. M., Pallares, F. J., Barranco, I., Carrasco, L., & Gómez-Laguna, J. (2020). Activation of the extrinsic apoptotic pathway in the thymus of piglets infected with PRRSV-1 strains of different virulence. *Veterinary Microbiology*, *243*, 108639. https://doi.org/10.1016/j.vetmic.2020.108639

Sánchez-Carvajal, J. M., Rodríguez-Gómez, I. M., Carrasco, L., Barranco, I., Álvarez, B., Domínguez, J., Salguero, F. J., & Gómez-Laguna, J. (2019). Kinetics of the expression of CD163 and CD107a in the lung and tonsil of pigs after infection with PRRSV-1 strains of different virulence. *Veterinary Research Communications*, *43*(3), 187–195. https://doi.org/10.1007/s11259-019-09755-x

Sánchez, C., Doménech, N., Alonso, F., Ezquerra, A., Domínguez, J., & Vázquez, J. (1999). The porcine 2A10 antigen is homologous to human CD163 and related to macrophage differentiation. *Journal of Immunology*, *162*(9), 5230–5237.

Schönrich, G., & Raftery, M. J. (2019). The PD-1/PD-L1 axis and virus infections: A delicate balance. In *Frontiers in Cellular and Infection Microbiology* (Vol. 9, p. 207). Frontiers Media S.A. https://doi.org/10.3389/fcimb.2019.00207

Shi, M., Lam, T. T. Y., Hon, C. C., Hui, R. K. H., Faaberg, K. S., Wennblom, T., Murtaugh, M. P., Stadejek, T., & Leung, F. C. C. (2010). Molecular epidemiology of PRRSV: A phylogenetic perspective. *Virus Research*, *154*(1–2), 7–17. https://doi.org/10.1016/j.virusres.2010.08.014

Sibila, M., Calsamiglia, M., Segalés, J., Blanchard, P., Badiella, L., Le Dimma, M., Jestin, A., & Domingo, M. (2004). Use of a polymerase chain reaction assay and

799 an ELISA to monitor porcine circovirus type 2 infection in pigs from farms with
800 and without postweaning multisystemic wasting syndrome. *American Journal of*
801 *Veterinary Research*, *65*(1), 88–92. https://doi.org/10.2460/ajvr.2004.65.88
802 Silva-Campa, E., Cordoba, L., Fraile, L., Flores-mendoza, L., Montoya, M., &
803 Hernández, J. (2010). European genotype of porcine reproductive and respiratory
804 syndrome (PRRSV) infects monocyte-derived dendritic cells but does not induce
805 Treg cells. *Virology*, *396*(2), 264–271. https://doi.org/10.1016/j.virol.2009.10.024
806 Silva-Campa, E., Flores-Mendoza, L., Reséndiz, M., Pinelli-Saavedra, A., Mata-Haro,
807 V., Mwangi, W., & Hernández, J. (2009). Induction of T helper 3 regulatory cells
808 by dendritic cells infected with porcine reproductive and respiratory syndrome
809 virus. *Virology*, *387*(2), 373–379. https://doi.org/10.1016/j.virol.2009.02.033
810 Singh, R., Alape, D., Lima, A. de, Ascanio, J., Majid, A., & Gangadharan, S. P. (2019).
811 Regulatory T Cells in Respiratory Health and Diseases. *Pulmonary Medicine*,
812 *2019*. https://doi.org/10.1155/2019/1907807
813 Sinn, L. J., Klingler, E., Lamp, B., Brunthaler, R., Weissenböck, H., Rümenapf, T., &
814 Ladinig, A. (2016). Emergence of a virulent porcine reproductive and respiratory
815 syndrome virus (PRRSV) 1 strain in Lower Austria. *Porcine Health Management*,
816 *2*, 1–10. https://doi.org/10.1186/s40813-016-0044-z
817 Snelgrove, R. J., Goulding, J., Didierlaurent, A. M., Lyonga, D., Vekaria, S., Edwards,
818 L., Gwyer, E., Sedgwick, J. D., Barclay, A. N., & Hussell, T. (2008). A critical
819 function for CD200 in lung immune homeostasis and the severity of influenza
820 infection. *Nature Immunology*, *9*(9), 1074–1083. https://doi.org/10.1038/ni.1637
821 Stadejek, T., Larsen, L. E., Podgórska, K., Bøtner, A., Botti, S., Dolka, I., Fabisiak, M.,
822 Heegaard, P. M. H., Hjulsager, C. K., Hućˊ, T., Kvisgaard, L. K., Sapierzyński, R.,
823 & Nielsen, J. (2017). Pathogenicity of three genetically diverse strains of PRRSV

824 Type 1 in specific pathogen free pigs. *Veterinary Microbiology*, *209*(April), 13–19.
825 https://doi.org/10.1016/j.vetmic.2017.05.011
826 Thanawongnuwech, R., Halbur, P. G., & Thacker, E. L. (2000). The role of pulmonary
827 intravascular macrophages in porcine reproductive and respiratory syndrome virus
828 infection. In *Animal health research reviews / Conference of Research Workers in*
829 *Animal Diseases* (Vol. 1, Issue 2, pp. 95–102).
830 https://doi.org/10.1017/S1466252300000086
831 Vaine, C. A., & Soberman, R. J. (2014). The CD200-CD200R1 Inhibitory Signaling
832 Pathway. Immune Regulation and Host-Pathogen Interactions. In *Advances in*
833 *Immunology* (Vol. 121, pp. 191–211). Academic Press Inc.
834 https://doi.org/10.1016/B978-0-12-800100-4.00005-2
835 Van Gorp, H., Van Breedam, W., Delputte, P. L., & Nauwynck, H. J. (2008).
836 Sialoadhesin and CD163 join forces during entry of the porcine reproductive and
837 respiratory syndrome virus. *Journal of General Virology*, *89*(12), 2943–2953.
838 https://doi.org/10.1099/vir.0.2008/005009-0
839 Van Gucht, S., Labarque, G., & Van Reeth, K. (2004). The combination of PRRS virus
840 and bacterial endotoxin as a model for multifactorial respiratory disease in pigs.
841 *Veterinary Immunology and Immunopathology*, *102*(3), 165–178.
842 https://doi.org/10.1016/j.vetimm.2004.09.006
843 Van Gucht, S., Reeth, K. Van, Nauwynck, H., & Pensaert, M. (2005). Porcine
844 Reproductive and Respiratory Syndrome Virus Infection Increases CD14
845 Expression and Lipopolysaccharide-Binding Protein in the Lungs of Pigs. *Viral*
846 *Immunology*, *18*(1), 116–126. https://doi.org/10.1089/vim.2005.18.116
847 Van Reeth, K., & Nauwynck, H. (2000). Proinflammatory cytokines and viral
848 respiratory disease in pigs. *Veterinary Research*, *31*(2), 187–213.

https://doi.org/10.1051/vetres:2000113

Vlahos, R., Stambas, J., Bozinovski, S., Broughton, B. R. S., & Drummond, G. R. (2011). Inhibition of Nox2 Oxidase Activity Ameliorates Influenza A Virus-Induced Lung Inflammation. *PLoS Pathog*, *7*(2), 1001271. https://doi.org/10.1371/journal.ppat.1001271

Wang, L., Wang, X., Tong, L., Wang, J., Dou, M., Ji, S., Bi, J., Chen, C., Yang, D., He, H., Bai, C., Zhou, J., & Song, Y. (2018). Recovery from acute lung injury can be regulated via modulation of regulatory T cells and Th17 cells. *Scandinavian Journal of Immunology*, *88*(5), e12715. https://doi.org/10.1111/sji.12715

Weesendorp, E., Morgan, S., Stockhofe-Zurwieden, N., Graaf, D. J. P. De, Graham, S. P., & Rebel, J. M. J. (2013). Comparative analysis of immune responses following experimental infection of pigs with European porcine reproductive and respiratory syndrome virus strains of differing virulence. *Veterinary Microbiology*, *163*(1–2), 1–12. https://doi.org/10.1016/j.vetmic.2012.09.013

Weesendorp, E., Rebel, J. M. J., Popma-De Graaf, D. J., Fijten, H. P. D., & Stockhofe-Zurwieden, N. (2014). Lung pathogenicity of European genotype 3 strain porcine reproductive and respiratory syndrome virus (PRRSV) differs from that of subtype 1 strains. *Veterinary Microbiology*, *174*(1–2), 127–138. https://doi.org/10.1016/j.vetmic.2014.09.010

Whitworth, K. M., Rowland, R. R. R., Ewen, C. L., Trible, B. R., Kerrigan, M. A., Cino-Ozuna, A. G., Samuel, M. S., Lightner, J. E., McLaren, D. G., Mileham, A. J., Wells, K. D., & Prather, R. S. (2016). Gene-edited pigs are protected from porcine reproductive and respiratory syndrome virus. *Nature Biotechnology*, *34*(1), 20–22. https://doi.org/10.1038/nbt.3434

Yan, M., Hou, M., Liu, J., Zhang, S., Liu, B., Wu, X., & Liu, G. (2017). Regulation of

874 iNOS-Derived ROS Generation by HSP90 and Cav-1 in Porcine Reproductive and
875 Respiratory Syndrome Virus-Infected Swine Lung Injury. *Inflammation*, *40*(4),
876 1236–1244. https://doi.org/10.1007/s10753-017-0566-9
877

878 **Figure Legends**

879 **Fig. 1. Clinical signs score, macroscopic and microscopic lung outcomes.** Clinical
880 signs and temperature were recorded from 1 day prior to infection until 8 dpi to evaluate
881 clinical signs and hyperthermia (> 40.5°C). Plots show the mean average of clinical signs
882 score **(A)** and rectal temperature **(B)** for control group (gray circles), 3249-infected group
883 (green triangle) and Lena-infected group (red diamonds). "a" indicates a significant
884 difference between the Lena and 3249 and control groups, "b" a significant difference
885 between the Lena and 3249 groups and "c" a significant difference between the 3249 and
886 control groups. *P* value lower than 0.05 was considered statistically significant and
887 represented as * $P \leq 0.05$, ** $P \leq 0.01$ and *** $P \leq 0.001$. Days post-inoculation, dpi. **(C)**
888 At necropsy, lungs were scored and processed for histological and immunohistochemical
889 studies. Box plots display the macroscopic lung score for each group (control, gray
890 circles; 3249, green triangles; Lena, red diamonds) for each time point. *P* value lower
891 than 0.05 was considered statistically significant and represented as * $P \leq 0.05$, ** $P \leq$
892 0.01 and *** $P \leq 0.001$. Days post-inoculation, dpi. **(D)** Lung appearance of piglets from
893 the control, 3249 and Lena group at 8 dpi are shown in the pictures. **(E)** Box plots show
894 the microscopic lung score for each group (control, gray circles; 3249, green triangles;
895 Lena, red diamonds) for each time point. Each symbol represents individual data for each
896 pig. *P* value lower than 0.05 was considered statistically significant and represented as *
897 $P \leq 0.05$, ** $P \leq 0.01$ and *** $P \leq 0.001$. Days post-inoculation, dpi. **(F)**
898 Photomicrographs of the medial lung lobe illustrate characteristic interstitial pneumonia
899 in a representative 3249-infected pig (left) and suppurative bronchopneumonia in a
900 representative Lena-infected pig (right) at 8 dpi. Haematoxylin and eosin. Bar, 100 μm.
901

Fig. 2. PRRSV viraemia, lung viral load, IFN-γ and IL-6 level in sera. PRRSV viral load was quantified in sera **(A)** and lung **(B)** by RT-qPCR. The concentration of IFN-γ **(C)** and IL-6 **(D)** were assessed in sera by using ELISA. Diagrams (**A**) and (**B**) display the viral load (eq $TCID_{50}$/mL) and (**C)** and (**D)** the concentration of the cytokines IFN-γ (pg/mL) and IL-6 (pg/mL), respectively, for each group (control, gray circles; 3249, green triangles; Lena, red diamonds) and time point. All data are reported as the mean with range of results obtained for each group and time point. *P* value lower than 0.05 was considered statistically significant and represented as * $P \leq 0.05$ and ** $P \leq 0.01$. "a" indicates a significant difference between the Lena and 3249 and control groups and "b" a significant difference between the 3249 and control groups. Days post-inoculation, dpi.

Fig. 3. Immunohistochemical expression of PRRSV-N-protein and CD163 in lung tissue. Lung tissue sections were immunolabelled for both antigens. Photomicrographs of the medial lung lobe illustrate the expression of PRRSV-N-protein in a 3249-infected (**A**) and Lena-infected (**B**) pig, which was mainly observed in PAMs (3A-3B, insets). IHC. Bar, 100 μm. Photomicrographs of the medial lung lobe illustrate the expression of CD163 in a representative control (**C**) and Lena-infected (**D**) pig. Immunolabelling of CD163 scavenger receptor was mainly observed in the cytoplasm and cell surface of PAMs found in the pulmonary alveolus and in a lesser extent in interstitial and intravascular macrophages (3C-3D, insets). IHC. Bar, 50 μm. **(E)** The diagram displays the number of PRRSV-N-protein$^+$ (primary axis) and CD163$^+$ (secondary axis) cells/mm^2. Scatter dot plot shows the number of CD163$^+$ macrophages (secondary axis) for each animal (control, gray circles; 3249, green triangles; Lena, red diamonds) and coloured lines the average for each group and time point. Control baseline displays the mean of the number of positive cells along the study in control group. *P* value lower than 0.05 was

927 considered statistically significant and represented as * $P \leq 0.05$ and ** $P \leq 0.01$. The
928 grey bars display the average of total number of PRRSV-N-protein^{+} macrophages
929 (primary axis) for each group and time point. “a” indicates a significant difference
930 between the Lena and 3249 groups. Days post-inoculation, dpi.
931
932 **Fig. 4. Immunohistochemical expression of CD14 and iNOS in lung tissue**. Lung
933 tissue sections were immunolabelled for both antigens. Photomicrographs of the medial
934 lung lobe illustrate the expression of CD14 in a 3249-infected (**A**) and Lena-infected pig
935 (**B**), which was mainly expressed on the cell membrane and cytoplasm of monocytes,
936 interstitial and intravascular macrophages (4A-4B, insets). IHC. Bar, 100 μm.
937 Photomicrographs of the medial lung lobe illustrate the expression of iNOS in a
938 representative control (C) and Lena-infected (D) pig. iNOS was observed primarily in the
939 cytoplasm of PAMs and interstitial macrophages detected in foci of interstitial pneumonia
940 and bronchopneumonia (4C-4D, insets). IHC. Bar, 100 μm. **(E)** Box plots shows the
941 number of CD14^{+} cells/mm^{2} for each group (control, gray circles; 3249, green triangles;
942 Lena, red diamonds) and time point. **(F)** Box plots display the number of iNOS^{+} cells for
943 each group (Control, gray circles; 3249, green triangles; Lena, red diamonds) and time
944 point. Control baseline displays the mean of the number of positive cells along the study
945 in control group. *P* value lower than 0.05 was considered statistically significant and
946 represented as * $P \leq 0.05$ and ** $P \leq 0.01$. Days post-inoculation, dpi.
947
948 **Fig. 5. Immunohistochemical expression of CD200R1 and FoxP3 in lung tissue.**
949 Lung tissue sections were immunolabelled for both antigens. Photomicrographs of the
950 medial lung lobe illustrate the expression of CD200R1 in a 3249-infected (**A**) and Lena-
951 infected (**B**) pig, which was mainly detected in the cytoplasm of intravascular and

interstitial macrophages located inside or surrounding bronchopneumonia foci (5A-5B, insets). IHC. Bar, 50 μm. Photomicrographs of the medial lung lobe illustrate the expression of FoxP3 in a representative control (**C**) and Lena-infected (**D**) pig. FoxP3 yielded a nuclear immunolabelling in lymphocytes mainly located in areas of atelectasis and interstitial pneumonia (5C-5D, insets). IHC. Bar, 100 μm. **(E)** The diagram displays the number of $CD200R1^+$ cells/mm^2 versus the microscopic lung score. Scatter dot plot shows the number of $CD200R1^+$ cells (primary axis) for each animal (control, gray circles; 3249, green triangles; Lena, red diamonds) and coloured lines the average for each group and day point. The gray bar displays the microscopic lung score (secondary axis) for each group (control, gray circles; 3249, green triangles; Lena, red diamonds) at each time point. **(F)** Box plots shows the number of $FoxP3^+$ cells for each group (control, gray circles; 3249, green triangles; Lena, red diamonds) and time point. Control baseline displays the mean of the number of positive cells along the study in control group. *P* value lower than 0.05 was considered statistically significant and represented as * $P \leq 0.05$ and ** $P \leq 0.01$. Days post-inoculation, dpi.

Highlights

- Lena virulent strain caused an increase in sera levels of IFN-γ and IL-6.
- Lung viral load and PRRSV-N-protein^{+} cells were inversely correlated with CD163^{+} macrophages in the lung.
- CD14^{+} cells infiltrated interstitium to possibly replenish macrophages subsets.
- Lena-induced microscopic lung injury was linked to an increase of iNOS^{+} cells.
- The increase of CD200R1^{+} and FoxP3^{+} cells was associated with the course of lung injury.

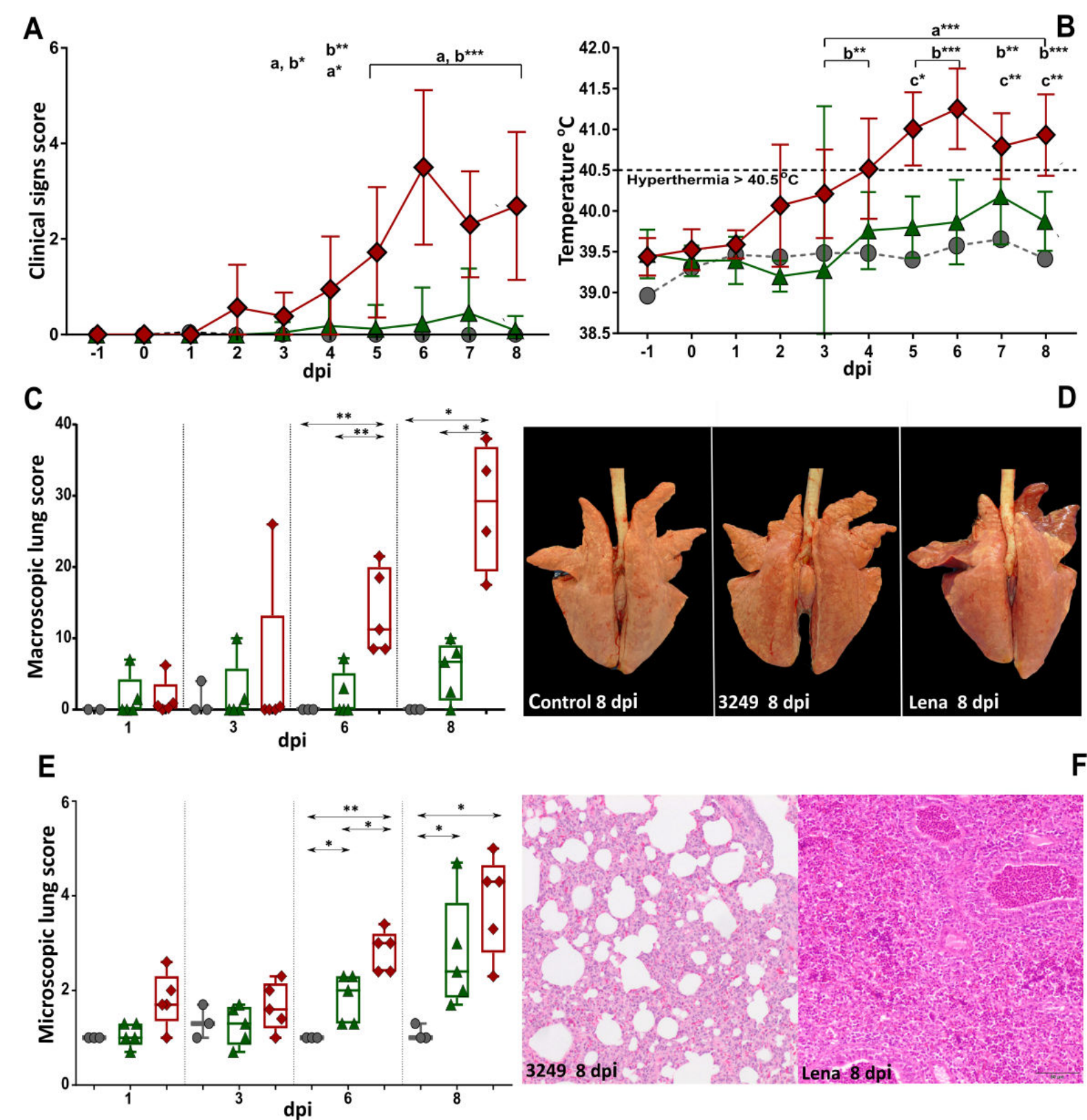
A
Clinical signs score
dpi
a, b*
b**
a*
a, b***
B
Temperature °C
Hyperthermia > 40.5°C
a***
b**
b***
b**
b***
c*
c**
c**
dpi
C
Macroscopic lung score
dpi
D
Control 8 dpi
3249 8 dpi
Lena 8 dpi
E
Microscopic lung score
dpi
F
3249 8 dpi
Lena 8 dpi

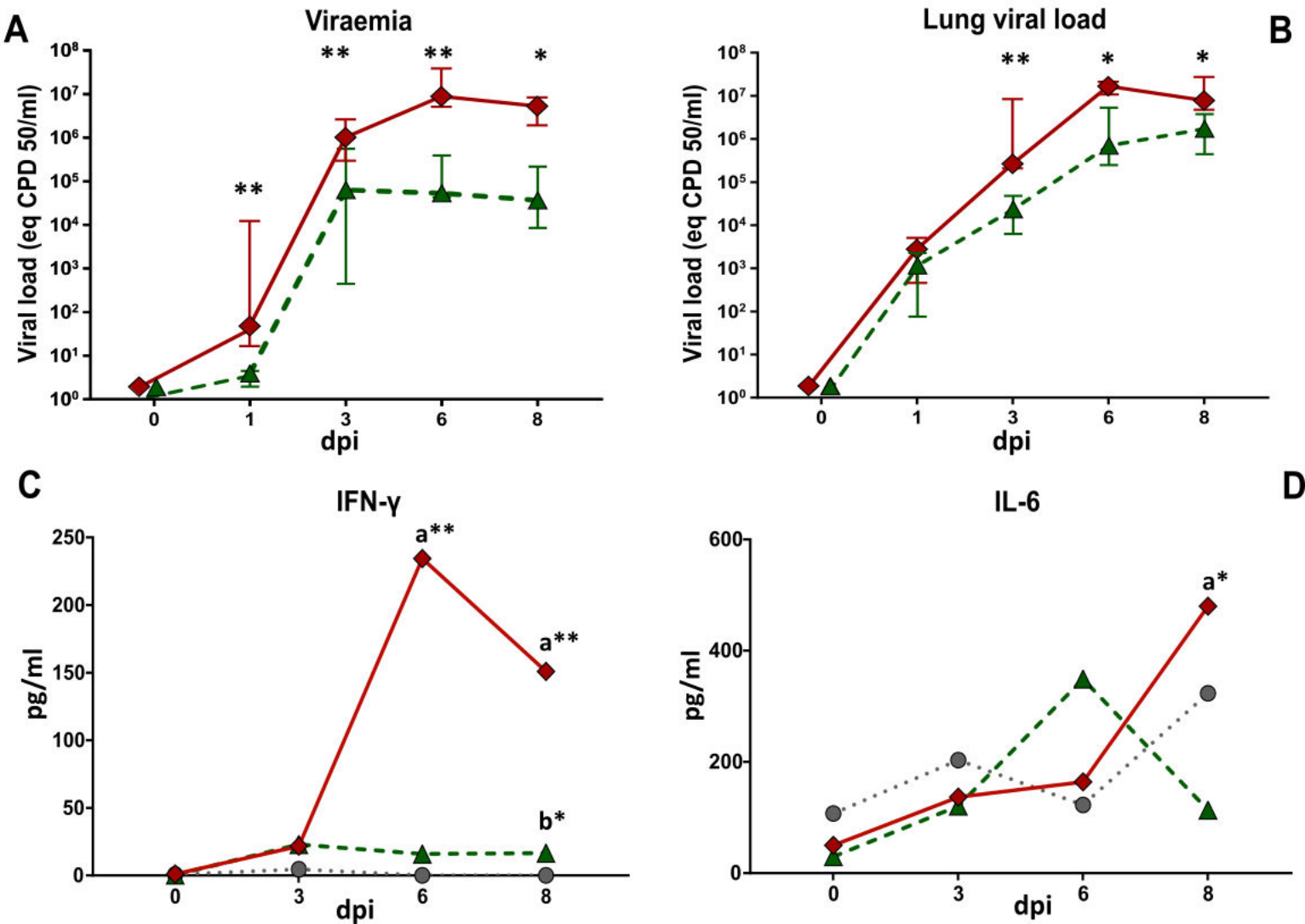
A
Viraemia
Viral load (eq CPD 50/ml)
dpi
B
Lung viral load
C
IFN-γ
pg/ml
a**
b*
D
IL-6
a*

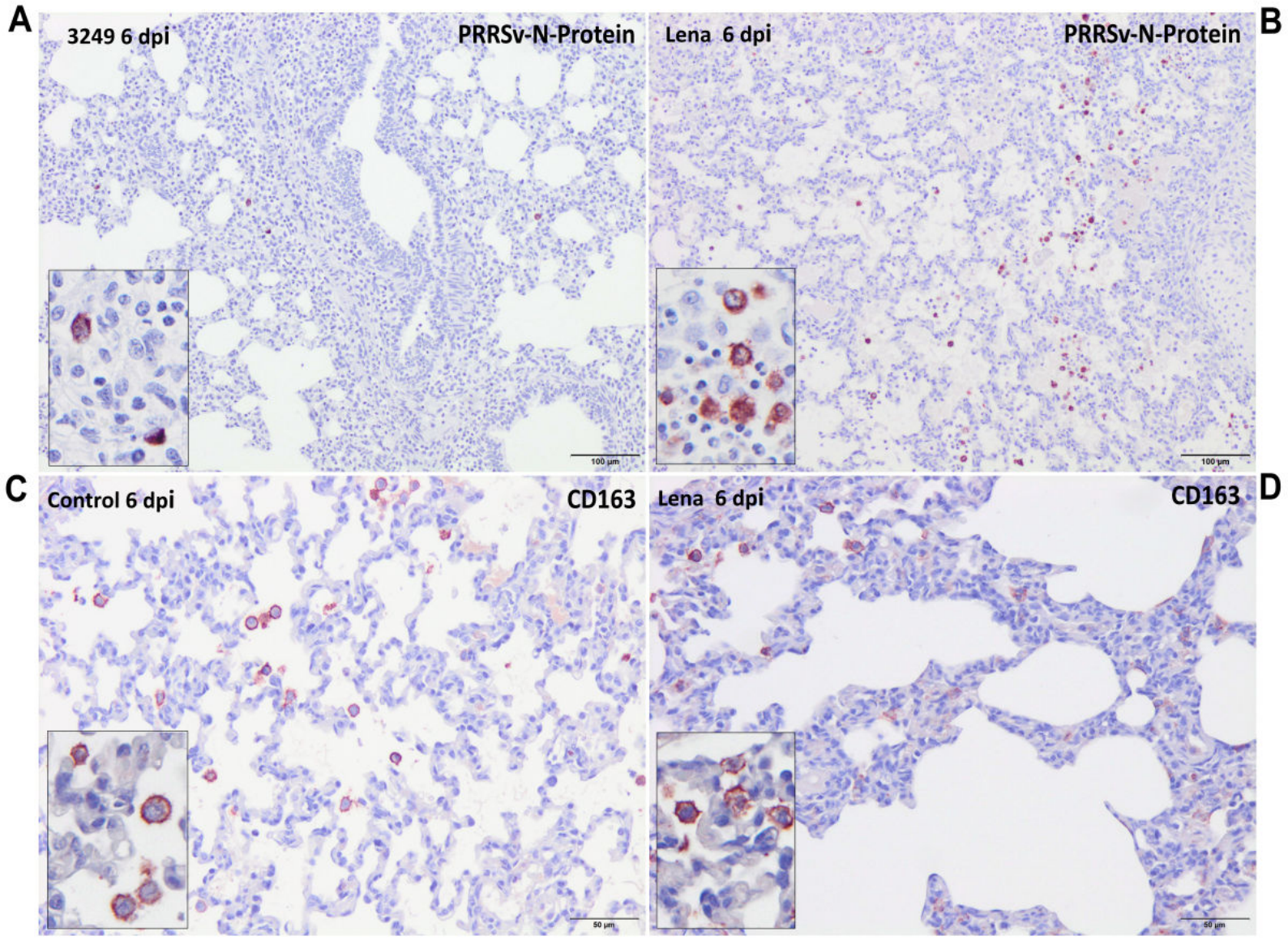
A
3249 6 dpi
PRRSv-N-Protein
B
Lena 6 dpi
PRRSv-N-Protein
C
Control 6 dpi
CD163
D
Lena 6 dpi
CD163

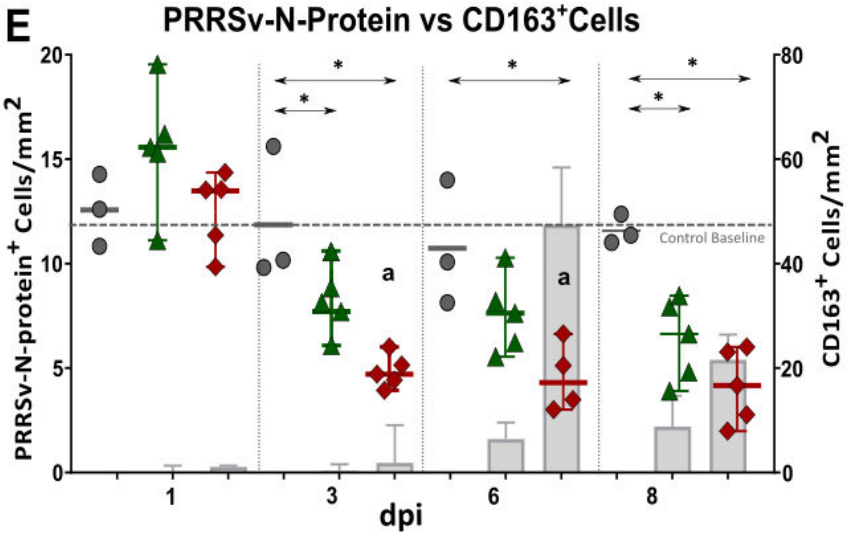
E
PRRSv-N-Protein vs CD163+Cells
PRRSv-N-protein+ Cells/mm2
CD163+ Cells/mm2
Control Baseline
a
a
dpi
1
3
6
8
0
5
10
15
20
0
20
40
60
80

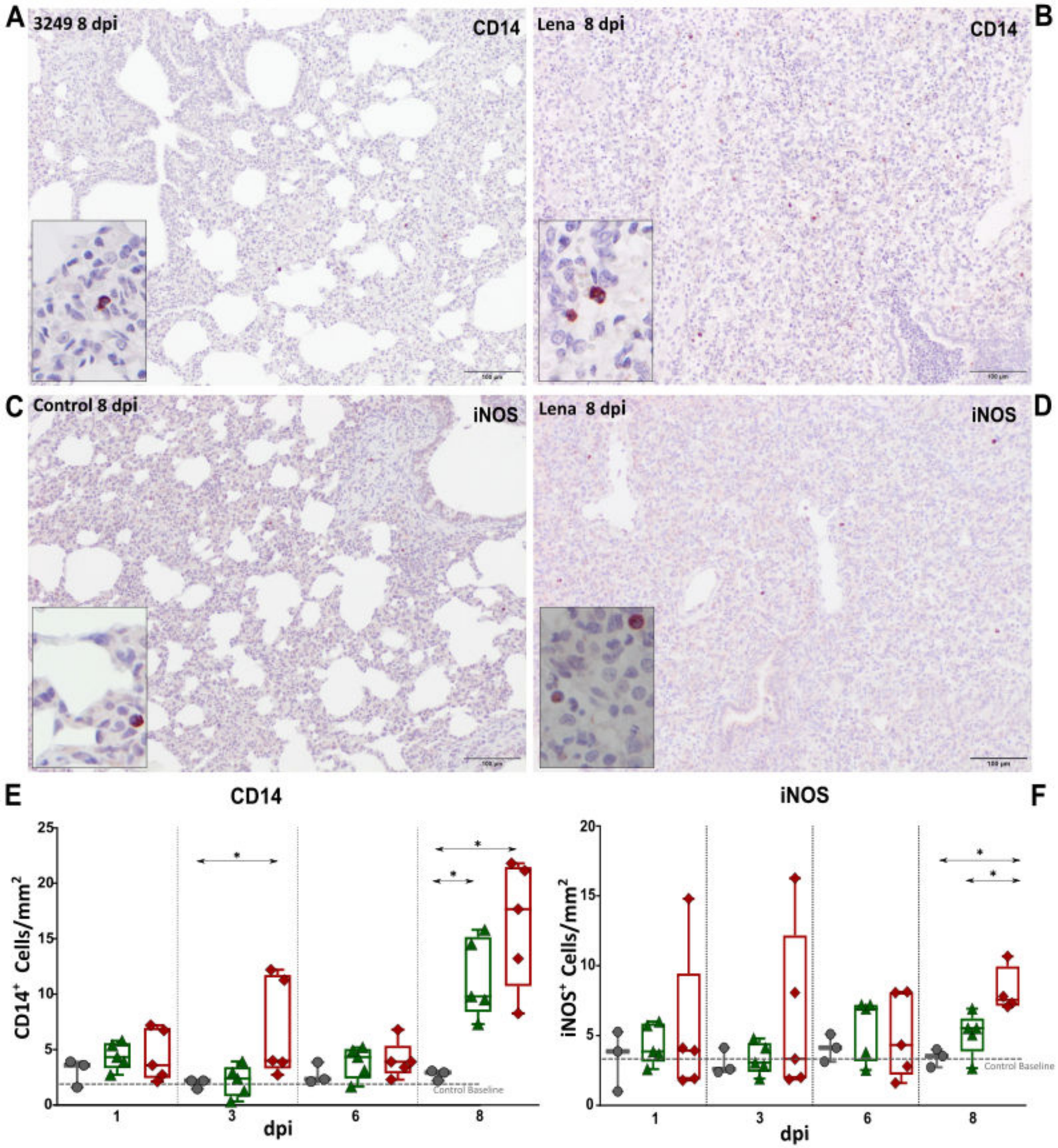
A
3249 8 dpi
CD14
B
Lena 8 dpi
CD14
C
Control 8 dpi
iNOS
D
Lena 8 dpi
iNOS
E
CD14
CD14⁺ Cells/mm²
25
20
15
10
5
0
1
3
6
8
dpi
Control Baseline
*
*
*
F
iNOS
iNOS⁺ Cells/mm²
20
15
10
5
0
1
3
6
8
dpi
Control Baseline
*
*

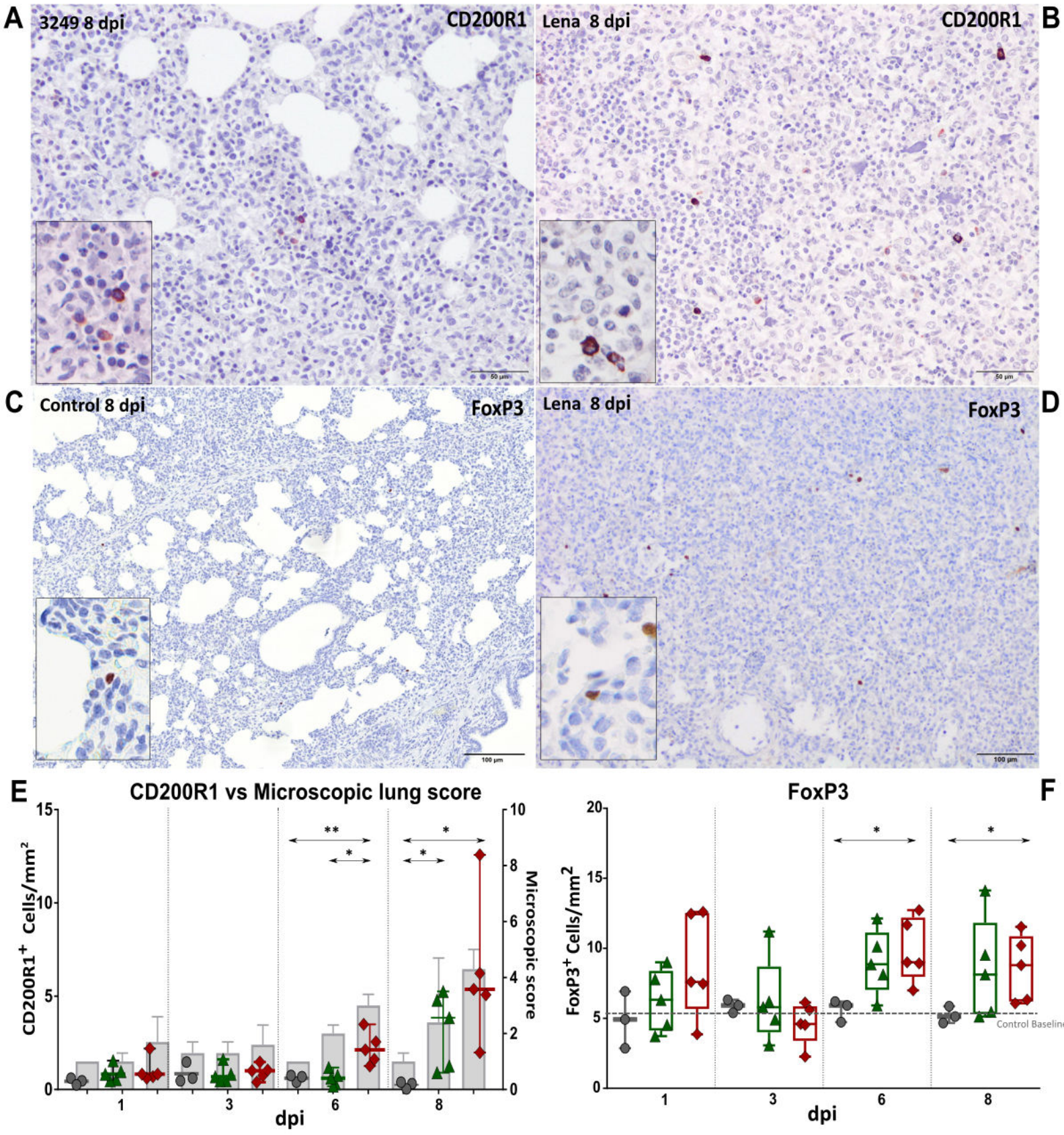
A
3249 8 dpi
CD200R1
B
Lena 8 dpi
CD200R1
C
Control 8 dpi
FoxP3
D
Lena 8 dpi
FoxP3
E
CD200R1 vs Microscopic lung score
CD200R1+ Cells/mm2
Microscopic score
dpi
F
FoxP3
FoxP3+ Cells/mm2
Control Baseline
dpi

Table 1. Summary of immunohistochemical methodology.

Specificity	Type of antibodies	Clone	Source	Blocking solution	Dilution	Antigen retrieval
PRRSV-N- protein	mAb	SDOW17	Rural Technologies, Brookings, SD, USA	BSA 2%	1:500	Protease XIV
CD163	mAb	2A10/11	In house, INIA	NGS 10%	neat	Citrate pH 6
CD200R1	mAb	PCT3	In house, INIA	BSA 2%	neat	Protease XIV
CD14	mAb	MIL2	Biorad, Hercules, CA	BSA 2%	1:100	Protease XIV
iNOS	pAb	NA	Neomarers, Fremont, CA, USA	BSA 2%	1:750	Citrate pH 6*
FoxP3	mAb	FJK-16s	eBioscience™, Bacelona, Spain	NGS 10%**	1:100	Citrate pH 6*

PRRSV, *Porcine reproductive and respiratory syndrome virus*; CD200R1, CD200 Receptor 1; iNOS, inducible nitric oxide synthase; FoxP3, forkhead box protein 3; mAb, monoclonal antibody; pAb, polyclonal antibody; BSA, Bovine Serum Albumin; NGS, Normal Goat Serum; NA, not applicable; Citrate pH 6, microwave heat treatment at 420W for 10 minutes; Protease XIV, enzymatic digestion with protease type XIV (Sigma-Aldrich) at 38º C for 8 minutes; Citrate pH 6*, autoclave treatment at 121º C for 10 min; NGS 10%**: NGS diluted in phosphate buffer saline with 10% tween 20.

Table 2. Statistical correlations found in piglets infected with virulent Lena strain throughout the study. For all data, a *P* value lower than 0.05 was considered statistically significant and represented as * $P \leq 0.05$, ** $P \leq 0.01$, *** $P \leq 0.001$ and **** $P \leq 0.0001$.

	Temperature	**Clinical score**	**Viraemia**	**Lung viral Load**	**IFN-γ**	**IL-6**	**Gross lesion**	**Microscopic lesion**	**PRRSV-N-protein**	**CD163**	**CD200R1**	**FoxP3**	**CD14**	**iNOS**
Temperature	-	0.92****	0.79****	0.76****	0.67*	NS	0.62**	0.64**	0.78****	NS	NS	NS	NS	NS
Clinical signs score		-	0.84****	0.72****	0.72***	NS	0.68**	0.75****	0.78****	NS	-0.63**	NS	NS	NS
Viraemia			-	0.77****	0.71**	NS	NS	0.62**	0.74**	-0.78***	NS	NS	NS	NS
Lung viral load				-	0.71***	NS	0.72***	0.68**	0.85****	-0.71***	0.63**	NS	NS	NS
IFN-γ					-	NS	NS	0.62*	0.62*	NS	0.61**	0.70**	NS	NS
IL-6						-	NS	NS	0.55*	NS	0.56*	NS	0.84***	NS
Gross lesion							-	0.8***	NS	NS	0.73***	NS	NS	NS
Microscopic lesion								-	0.68**	NS	0.91****	NS	NS	NS
PRRSV-N-protein									-	-0.62**	0.63**	NS	NS	NS
CD163										-	NS	NS	NS	NS
CD200R1											-	NS	0.55*	NS
FoxP3												-	NS	NS
CD14													-	0.52*
iNOS														-

NS: not statistically significant or with r < 0.6. Correlation coefficients were considered relevant with r > 0.6 and $P < 0.05$.